THE ASTROPHYSICAL JOURNAL, 315:706–715, 1987 April 15

SOLAR WIND DIAGNOSTICS FROM DOPPLER-ENHANCED SCATTERING

GIANCARLO NOCI
Istituto di Astronomia, Università di Firenze

AND

JOHN L. KOHL AND GEORGE L. WITHBROE
Harvard-Smithsonian Center for Astrophysics
Received 1986 January 20; accepted 1986 September 30

ABSTRACT

Solar wind ions can attain sufficient outflow speed, w, to cause line excitation by chromospheric or transition region radiation in a nearby line. We show that this extends the diagnostic possibilities of a coronal EUV line to much larger values of w than would be possible if pumping were limited to radiation from the same spectral line. For the $\lambda 1037.6$ coronal line of O VI, the pumping effect of the chromospheric C II $\lambda 1037.0$ line is efficient for $100 < w < 250$ km s^{-1}. We derive an approximate expression for the line ratio for a doublet of the Li or Na isoelectronic sequences and discuss the diagnostic capabilities of doublet line ratios, either by themselves or combined with the observation of other quantities. In particular, we show that the determination of doublet line ratios at several heights can be sufficient to yield the solar wind velocity at those heights together with a constraint on other coronal parameters.

Subject headings: plasmas — Sun: corona — Sun: solar wind — Sun: spectra — ultraviolet: spectra

I. INTRODUCTION

The possibility of using the Doppler dimming effect (Hyder and Lytes 1970) as a diagnostic tool to measure outflow velocities in the extended solar corona has been discussed in several papers (Beckers and Chipman 1974; Withbroe *et al.* 1982) and an observational program has been devised (Kohl *et al.* 1980) which utilizes an UV coronal spectrometer and a white-light coronagraph to perform this and other plasma diagnostic techniques in the absence of a natural solar eclipse. A discussion of the utility of H I Lyα and of other solar lines for the determination of physical parameters, such as the solar wind outflow speed, the ion temperature and the electron density, is the subject of a paper by Kohl and Withbroe (1982). A result of their study is that the O VI resonance doublet at 1032 Å and 1037 Å is a promising tool for the investigation of the low-speed (30–80 km s^{-1}) solar wind.

For the usual case of Doppler dimming, the velocity sensitivity range is determined by the wavelength and width of the spectral line of interest. The highest velocity sensitivity available for the simple Doppler dimming effect is ~ 300 km s^{-1} for H I Lyα. However, diagnostics for an arbitrarily large range of outflows are possible when pumping by neighboring lines is also considered. This capability becomes very important for high-speed coronal transient events that might otherwise Doppler-dim resonantly scattered intensities to an unmeasurable value. It is also important at lower speeds since it provides a check on velocity determinations based on simple Doppler dimming of Lyα; this occurs, for example, when one member of the O VI doublet is pumped by the C II $\lambda 1037.0$ line, since a velocity sensitivity in the 100–250 km s^{-1} range arises in that case.

The present paper describes this effect, namely, radiative excitation of a line by chromospheric or transition region photons in a nearby line. This phenomenon is an extension of Doppler dimming, which can be described in the following way. In the frame of reference of the outflowing solar wind, the spectrum originating in the chromosphere and transition region appears to be redshifted, hence the radiative excitation rate of a coronal line depends on the quantity:

$$F(\delta\lambda) = \int_0^\infty I_{\rm ex}(\lambda - \delta\lambda)\Phi_{\rm cor}(\lambda - \lambda_0)d\lambda\ , \qquad (1)$$

where λ is the wavelength, $\delta\lambda$ is the redshift, $I_{\rm ex}(\lambda)$ is the lower atmosphere intensity, $\Phi_{\rm cor}(\lambda - \lambda_0)$ is the normalized coronal absorption profile, and λ_0 is the wavelength at the line center.

It is clear that, if the lower atmospheric line is a simple emission line, i.e., if $I_{\rm ex}(\lambda)$ is maximum at the line center where $\Phi_{\rm cor}$ is also maximum, then $F(\delta\lambda)$ decreases as $\delta\lambda$ increases. Clearly, $F(\delta\lambda)$ would go to zero when $\delta\lambda \gg (\sigma_e + \sigma_a)/2$, where σ_e and σ_a are the widths of the lower atmospheric exciting line and of the coronal absorption profile, respectively, provided that the lower atmospheric radiation in the neighborhood of the considered line is negligible. If, however, a second emission line in the lower atmospheric spectrum is near to the violet wing of the line considered, then $F(\delta\lambda)$ increases again when $\Phi_{\rm cor}$ begins to overlay the second line. In practice, it will be interesting to consider those cases in which the wavelength separation of the neighboring line is small enough to correspond to reasonable values for coronal expansion speeds ($\delta\lambda = 0.33$ Å at $\lambda = 1000$ Å for an expansion speed of 100 km s^{-1}).

As we will see in § III, the case in which the enhanced coronal line belongs to a resonance doublet is the most significant. Although in this paper we will concentrate on the O VI doublet at 1032 Å and 1037.6 Å (where the latter can be pumped by C II $\lambda 1037.0$), an inspection of the solar EUV spectrum (Vernazza and Reeves 1978) reveals other resonance doublets which are expected to have one or both lines enhanced via Doppler-shifted radiation. Those which belong to the most abundant coronal ions are $\lambda 335.407$ and $\lambda 360.798$ of Fe XVI (the first line can be excited by Mg VIII $\lambda 335.0$ for a solar wind speed w of 364 km s^{-1} and the second by Fe XII $\lambda 359.7$ ($w = 913$ km s^{-1}) and Si XI $\lambda 359.0$ ($w = 1500$ km s^{-1}) and Mg x λ609.76 and λ624.93 [the first excited by O VI λ608.0 ($w = 866$ km s^{-1})].

In § II we provide an expression for the emissivity of the scattered component of a resonance line and show the effect of Doppler dimming, taking as a reference the case of the O VI λ1032 and λ1037.6 lines. For the latter we include the excitation due to the C II λ1037.0 chromospheric line.

In § III we study the dependence of the intensity ratio of two lines of a resonance doublet on the physical parameters of the coronal plasma. By using the expressions found in § II for the scattered components and standard expressions for the collisionally excited components, we work out a simple formula, equation (8), containing a parameter θ (which depends on electron density, electron temperature, kinetic temperature of the ion considered, the lower atmospheric exciting spectrum, and the dilution factor) and the Doppler factors of the two lines (which, to a good approximation, depend on the coronal expansion speed only). We also work out an expression, equation (14), that contains, in addition to the Doppler factors and a geometrical factor (equal to 1 for radial flow), only a parameter η, which for steady coronal expansion is independent, to a good approximation, of the heliocentric distance. This property makes this formula particularly useful for the diagnostics.

Equations (8) and (14) illustrate the following physical point: the proportion between collisional and radiative components of a resonance line depends on various physical parameters. If there are no nearby exciting lines, the intensity ratio of the two lines of a resonance doublet is expected to be intermediate between the ratio of the statistical weights and the intensity ratio squared (eqs. [9]–[10] of Kohl and Withbroe 1982). If, however, a nearby exciting line is present, the line emissivity ratio can go beyond those limits, and this effect depends on the expansion speed only. In other words, if the line ratio is outside those limits, at least a lower limit for the outflow speed is immediately obtained.

In § IV we study the best way of applying the expressions worked out in §§ II and III, to obtain information on the physical parameters of the coronal plasma. We treat various cases which depend on the kind of information available in addition to the measured intensity of the two lines considered. For the sake of simplicity and clarity, § III uses several approximations that would not be used directly for the interpretation of observational data. However, the approximate expressions serve to illustrate the versatility and sensitivity of diagnostic techniques based on Doppler-enhanced scattering. To obtain refined values, the ones from the approximate expressions should be used as starting points in detailed coronal models in which the doublet intensity ratio becomes the primary constraint on outflow velocity.

II. THE EMISSIVITY OF THE O VI λ1037.6 LINE

As shown in the appendix (eq. [A3]), the emissivity for the resonantly scattered component of a line, at a coronal point P, is given by

$$j(P, \boldsymbol{n}) = \frac{B_{12}\lambda_{12}h}{4\pi}\frac{N_1 G}{r^2}, \quad (2)$$

with

$$G = r^2 \int_{\Omega} p(\phi)F(\delta\lambda)d\omega', \quad (3)$$

where h is Plank's constant, B_{12} is the Einstein coefficient for

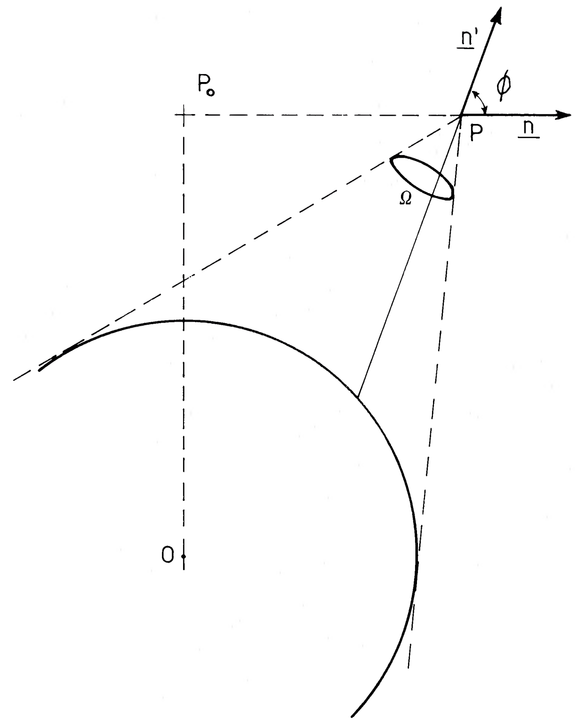

FIG. 1.—Geometry of the scattering process

absorption, λ_{12} is the wavelength of the considered transition, N_1 is the number density of scattering ions in the ground level, r the heliocentric distance, and $\boldsymbol{n}$ the unit vector parallel to the line of sight, directed toward the observer (Fig. 1). The integral over ω' takes into account the photons incident on P from different directions (defined by the unit vector $\boldsymbol{n}'$), ϕ is the angle between $\boldsymbol{n}$ and $\boldsymbol{n}'$, $p(\phi)$ gives the angular dependence of the scattering, and Ω is the solid angle subtended by the source of exciting radiation. The Doppler shift $\delta\lambda$ has the expression

$$\delta\lambda = \lambda \frac{\boldsymbol{w} \cdot \boldsymbol{n}'}{c},$$

where $\boldsymbol{w}$ is the coronal outflow velocity, so that it depends on the direction of the incoming radiation.

Following Kohl and Withbroe (1982) we define the Doppler factor

$$\mathrm{D} = \frac{\int_{\Omega} F(\delta\lambda)p(\phi)d\omega'}{\int_{\Omega} F(0)p(\phi)d\omega'}, \quad (4)$$

which is given as a function of the coronal outflow speed in Figure 2 of Kohl and Withbroe for several spectral lines. The plots of Kohl and Withbroe refer to the coronal point P_0, where the line of sight is perpendicular to the direction P_0-0 (0 is the Sun center) (Fig. 1) and assume radial outflow. They also assume that the intensity of the lower atmospheric spectrum is negligible at the near sides of the lines considered. However, this is not true for the O VI line at $\lambda = 1037.613$ Å (here and in the rest of this paper we take the wavelength values from Kelly and Palumbo 1973), which is an example of a case where a neighboring line, C II λ1037.018, exists at the right position for redshifts from reasonable outflow velocities to permit pumping of O VI ions to the upper level of the 1037.613 Å transition.

To determine the Doppler factor in this case it is necessary to know the lower atmospheric relative intensities of C II

λ1037.018 and O VI λ1037.613. The two lines are blended in the data obtained by the Harvard spectrometer on board *Skylab*. In spite of this the intensity of each line can be estimated in the following way. The O VI lines belong to a doublet: the transitions are $2s\ ^2S_{1/2}$–$2p\ ^2P_{1/2}$ (1037.6 Å) and $2s\ ^2S_{1/2}$–$2p\ ^2P_{3/2}$ (1032 Å). Owing to the much larger density in the transition region compared with that in the corona, the radiative contribution to the population of the $2p$ levels is negligible and thus the $2p$ levels are collisionally excited from the ground level. Accordingly, the population, and so the emissivity, of the $^2P_{3/2}$ level is twice that of the $^2P_{1/2}$ level. Since the transition region is effectively thin in the 1032 Å and 1037 Å lines, all photons emitted in these lines in a volume element within the transition region escape from this region (Pottasch 1964). Hence the intensity of the former line will be twice that of the latter (Kohl and Withbroe 1982). We can thus deduce the transition region intensity of the O VI λ1037.6 line from the *Skylab* observations (Vernazza and Reeves 1978) to be half the intensity observed for the 1032 Å line and finally obtain that of the C II component by subtracting the deduced O VI intensity from the observed blend at $\lambda = 1037$ Å. For a quiet region it turns out that I_{ex} (O VI λ1032) = 305, I_{ex} (O VI λ1037.6) = 152.5 and I_{ex} (C II λ1037.0) = 52 ergs cm^{-2} s^{-1} sr^{-1}. [The contribution from the continuum over the coronal absorption width is only 3% for the weakest (C II) line, and it is here neglected.]

At this point we need also to know the shape of the lower atmospheric exciting lines. The data available indicate a Gaussian shape for both the O VI and the C II lines with widths larger than the Doppler ones which correspond to the temperatures of maximum concentration of O VI and C II, respectively. There probably is a further broadening due to turbulent speed (23 km s^{-1} for O VI, 20 km s^{-1} for C II; Moe and Nicolas 1977), so that the O VI line would have a e^{-1} half-width of 0.101 Å and the C II line one of 0.072 Å. (We have taken the temperatures of formation from Jordan 1969.)

Finally, we assume a Gaussian shape for the coronal absorption profile, and we calculate equation (4) for the point P_0 defined above, at the heliocentric distances $r = \infty$ and $r = 2\ R_\odot$ ($R_\odot$ is the solar radius), and for the kinetic temperatures $T_k = 1 \times 10^6$ K and $T_k = 2 \times 10^6$ K. The results are given in Figure 2 for the λ1037.6 (D_{12}) and λ1032 (D_{13}) O VI lines.

Note, in Figure 2, the importance of the secondary maximum of the quantity D_{12}, which is due to pumping from the chromospheric C II line, and the fact that it occurs at a rather large outflow speed, compatible, however, with solar wind speeds at a few solar radii of heliocentric distance. We therefore expect an enhanced population of the O VI $2p\ ^2P_{1/2}$ state in the coronal regions where the solar wind originates.

Figure 2 shows the effect of the kinetic temperature on the Doppler factors as well as the effect of the heliocentric distance. It appears clearly that these two variables affect somewhat the velocity interval where the Doppler factors differ significantly from zero but do not influence their general character.

III. DOUBLETS

The diagnostic capability of the phenomenon described in the previous sections is the greatest when the line in question belongs to a resonance doublet of the Li or Na isoelectronic sequence, because in this case the second line provides an internal calibration and furthermore the population of the two upper levels are straightforward to obtain. Therefore we will concentrate on the intensity ratio of a coronal doublet of the Li or Na isoelectronic sequence beginning with the study of its dependence on the various physical parameters.

For radiation originating in an optically thin medium the

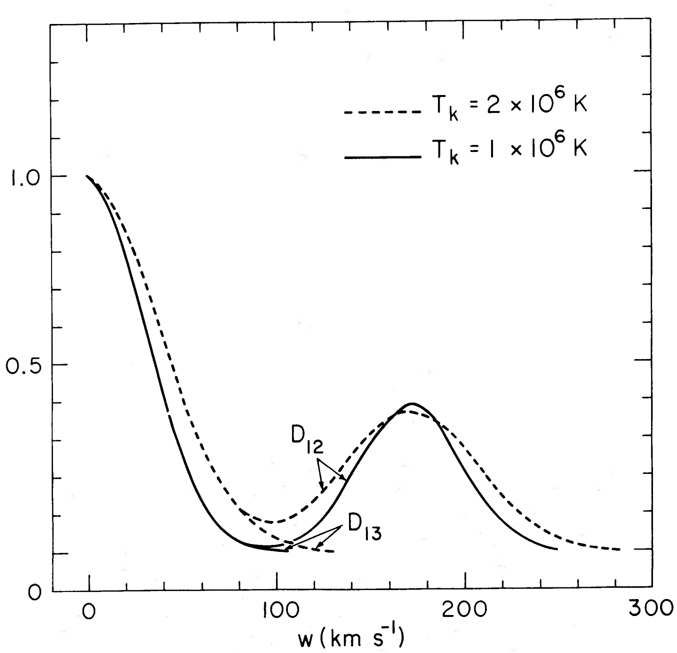

FIG. 2*a*

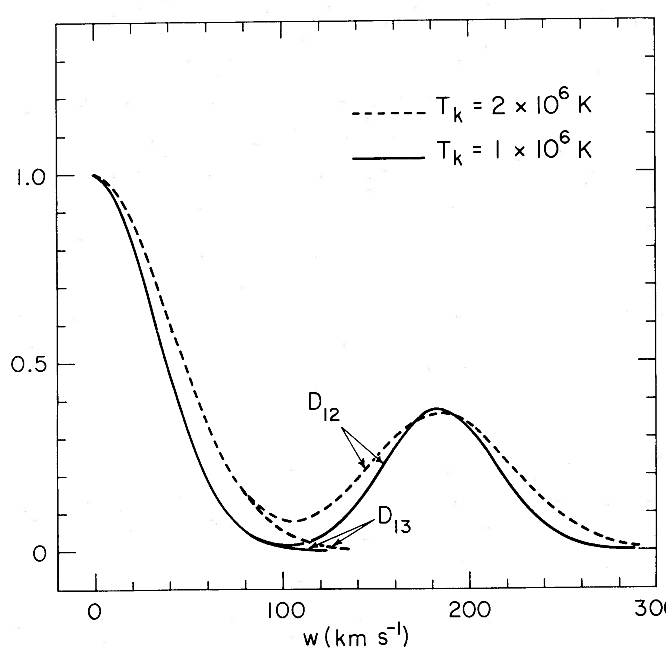

FIG. 2*b*

FIG. 2.—Doppler dimming of coronal O VI ions. Here D_{12}, D_{13} represent the normalized emissivity for the 1037.6 Å and 1032 Å lines, respectively (*see text*); *w* is the coronal outflow speed and T_k the ion kinetic temperature. (*a*) Asymptotic expressions (eq. [A6]) corresponding to $r = \infty$. (*b*) Exact expressions (eq. [4]) for $r = 2R$. The chromosphere and transition region are assumed here uniformly bright; the calculations refer to the point along the line of sight with $x = 0$ (*see text*).

ratio of the intensities of the two lines of the doublet is given by

$$\frac{I_{12}}{I_{13}} = \frac{\int_{-\infty}^{\infty} (h\nu_{12} C_{12} N_1/4\pi + j_{12})dx}{\int_{-\infty}^{\infty} (h\nu_{13} C_{13} N_1/4\pi + j_{13})dx} = \frac{\langle C_{12} N_1 + 4\pi j_{12}/h\nu_{12}\rangle}{\langle C_{13} N_1 + 4\pi j_{13}/h\nu_{13}\rangle},$$

where the x-axis starts at the point P_0 (Fig. 1) and runs along $\boldsymbol{n}$. Here C_{ik} is the collisional excitation rate from level i to level k, ν_{ik} is the frequency of the ik transition, and j_{ik} is the quantity defined in equation (2); the ground level is indicated by suffix 1, the lower level of the doublet by suffix 2, and the upper level of the doublet by suffix 3. This equation assumes that the population of the 2 and 3 levels is due to excitation from the ground level and that the primary mechanism of de-excitation is radiative decay (see, e.g., Pottasch 1964; Noci 1971). It is also assumed that $\nu_{12} = \nu_{13}$.

The region of maximum contribution to the integral in the numerator can be different from that to the integral in the denominator, depending on the density and velocity distributions in the corona. A proper calculation of the intensity ratio, therefore, requires a coronal model. However, for the pupose of this discussion it is sufficient to approximate the ratio of the mean values with the ratio of the true values at $x = 0$, owing to the fact that the weighting function N_1 has its maximum value at $x = 0$ in a spherically symmetric corona. Therefore in the following discussion we will consider the ratio between the emissivities,

$$\rho = \frac{C_{12} N_1 + 4\pi j_{12}/h\nu_{12}}{C_{13} N_1 + 4\pi j_{13}/h\nu_{13}}, \tag{5}$$

at the point $P_0(x = 0)$, rather than that between their mean values (equal to the intensity ratio).

We will furthermore assume $\boldsymbol{w}$ to be radial and the lower atmosphere to be uniformly bright in the exciting radiation, so that the quantity G defined in equation (3) becomes a function of r and w only, $G = G(r, w)$. Since, as shown in the Appendix and by the comparison of Figures 2a and 2b, the explicit dependence of G on r is not large, we will sometimes use the approximation $G(r, w) = G(\infty, w)$ (eq. [A5]). This approximation is particularly good when $w = 0$.

We now transform equation (5) taking j_{ik} from equation (2) and putting $C_{ik} = N_e q_{ik}(T_e)$; q_{ik}, N_e, and T_e being respectively the electron impact excitation coefficient, the electron density, and temperature. Defining

$$\theta = \frac{\lambda_{13}^2 B_{13} G_{13}(r, 0)}{N_e q_{13} r^2 c}, \tag{6}$$

and recognizing that $q_{12}/q_{13} = B_{12}/B_{13} = g_2/g_3$ (g_2 and g_3 being the statistical weights of levels 2 and 3, respectively), equation (5) becomes

$$\rho = \frac{g_2}{g_3} \frac{1 + [G_{12}(r, 0)/G_{13}(r, 0)]\theta \mathrm{D}_{12}}{1 + \theta \mathrm{D}_{13}}, \tag{7}$$

where the D_{jk}'s are the quantities defined in equation (4). The parameter θ represents the ratio between radiative and collisional components of the 1–3 line for the case of negligible Doppler dimming; it is a dimensionless quantity.

It is interesting to calculate representative values of θ. Since we do not expect the electron temperature to vary much along the first few radii of heliocentric distance within a coronal feature, q_{13} will also vary little. The same is true for $G_{13}(r, 0)$, hence θ will vary approximately as $(N_e r^2)^{-1}$. We calculate θ using cgs units: $q_{13} = 2.73 \times 10^{-15}\ f_{13}\bar{g}\ \exp\ (-E_{13}/kT_e)/[E_{13}(T_e)^{1/2}]$, where k is Boltzmann's constant and $\bar{g}$ an effective Gaunt factor (Seaton 1964), and $B_{13} = 0.3335 f_{13}/E_{13}$, where f_{13} is the oscillator strength and E_{13} the energy difference between levels 1 and 3. We evaluate $G_{13}(r, 0)$ by using approximation (A4) and taking for the exciting lower atmospheric line a Gaussian shape with e^{-1} half-width $\Delta\lambda_{\mathrm{ex}}$, namely:

$$G_{13}(r, 0) = \frac{R_\odot^2 \int_{13} I_{\mathrm{ex}}(\lambda)d\lambda}{4\sqrt{\pi}(\Delta\lambda_{\mathrm{cor}}^2 + \Delta\lambda_{\mathrm{ex}}^2)^{1/2}}\, h(r),$$

where $\Delta\lambda_{\mathrm{cor}}$ is the e^{-1} half-width of the coronal absorption profile and the integral includes the whole exciting line. The quantity $h(r) = \Omega r^2/\pi R_\odot^2$ decreases rapidly from 2 at $r = R_\odot$ and approaches unity at large r; it is already down to 1.15 at $r = 1.5\, R_\odot$. Hence, in cgs units

$$\theta = 5.75 \times 10^2 \frac{\lambda_{13}^2 \exp(E_{13}/kT_e)\sqrt{T_e} \int_{13} I_{\mathrm{ex}}(\lambda)d\lambda}{\bar{g} N_e(\Delta\lambda_{\mathrm{cor}}^2 + \Delta\lambda_{\mathrm{ex}}^2)^{1/2}} \left(\frac{R_\odot}{r}\right)^2 h(r).$$

As a numerical example we compute θ for the $\lambda\lambda$1032, 1037 doublet of O VI in the quiet corona. We then have $\lambda_{13} =$ 1031.912 Å, $E_{13} = 1.9251 \times 10^{-11}$ ergs, $g_3 = 4$, $g_2 = 2$; the value of the Gaunt factor $\bar{g}$ is taken to be 1.13 (Bely 1966). For the electron and kinetic temperatures (the latter including both thermal and nonthermal contributions) we use 1.6×10^6 K, and for the other quantities the same values as in § II. Also, we put, at the coronal base, $N_e = 10^9\ \mathrm{cm}^{-3}$.

Accordingly, we get the quiet corona value $\theta = 0.0264$ at $r = R_\odot$. A representative coronal hole value is $\sim$6 times larger (density is 10 times smaller, exciting intensity is 1.6 times smaller, and electron and kinetic temperature variations almost compensate each other), while an active region value should not differ much from the quiet one since the increase in the density could be totally compensated by the exciting intensity; electron and kinetic temperature variations probably almost compensate each other also in this case (lower atmospheric data from Vernazza and Reeves 1978).

At larger heliocentric distances the lower atmospheric zone entering the field of view of the absorbing ions will include regions of different activity. This will make the $G(r, 0)$ factors appropriate to different features converge somewhat. The increase of θ due to the factor N_e^{-1} is the largest for coronal holes.

If the exciting lines are effectively thin in the sense described in § II, the intensity ratio of the exciting lower atmospheric lines is equal to the ratio between the statistical weights of the 2p levels. In this case $G_{12}(r, 0)/G_{13}(r, 0) = g_2/g_3$ and equation (7) becomes

$$\rho = \frac{g_2}{g_3} \frac{1 + (g_2/g_3)\theta \mathrm{D}_{12}}{1 + \theta \mathrm{D}_{13}}. \tag{8}$$

To discuss the variation of ρ with the heliocentric distance it is useful to distinguish the following two cases.

a) Regions with Negligible Outflow

In this case $\mathrm{D}_{12} = \mathrm{D}_{13} = 1$, whence

$$\rho = \frac{g_2}{g_3} \frac{1 + (g_2/g_3)\theta}{1 + \theta},$$

where the variation of ρ with the heliocentric distance is contained in θ only.

To understand the behavior of ρ as the heliocentric distance varies, one needs to know the variation of θ with r. As said above θ varies approximately as $h(r)/(N_e r^2)$. In a static corona with a temperature of 1.6×10^6 K, the density scale height is less than 0.15 $R_\odot$, so θ increases as r increases, and ρ decreases ($g_2 < g_3$). For the quiet corona value of θ calculated above the collisional components of the lines of the O VI doublet are dominant and ρ reaches its high-density limit, namely,

$$\rho(\theta \to 0) = g_2/g_3 . \tag{9}$$

Using the density data given by Allen (1973) for the maximum of activity, which is appropriate for a static corona, the low-density limit of ρ,

$$\rho(\theta \to \infty) = (g_2/g_3)^2 , \tag{10}$$

is not yet reached at $r = 2\ R_\odot$ ($\theta = 1.068$, $\rho = 0.371$), beyond which it is difficult to think of a static corona. Hence, in a static coronal region, the emissivity ratio decreases with increasing height from the collisional limit (eq. [9]) toward the radiative limit (eq. [10]). For the O VI doublet, the minimum value of the emissivity ratio within the static feature is larger than the latter limit.

b) Regions with Significant Outflow

This case is of greater interest, because of its potential use as an outflow diagnostic technique. To study it we introduce the quantity

$$F = N_e w r^2 f , \tag{11}$$

which represents the total particle flux (s^{-1}) through a cross section of a velocity tube and is therefore independent of r. Here f = constant if the coronal expansion is radial; otherwise $f = f(r)$. Putting equation (11) in equation (6) gives:

$$\theta = \frac{\lambda_{13}^2 B_{13} G_{13}(r, 0)}{c q_{13} F} f w . \tag{12}$$

Defining

$$\eta = \frac{\theta}{f w} = \frac{\lambda_{13}^2 B_{13} G_{13}(r, 0)}{c q_{13} F} , \tag{13}$$

we get

$$\rho = \frac{g_2}{g_3} \frac{1 + (g_2/g_3)\eta f w \mathrm{D}_{12}}{1 + \eta f w \mathrm{D}_{13}} . \tag{14}$$

Doing this we have used w rather than N_e as a variable and have almost eliminated the explicit dependence on r, so that ρ depends on r almost only through the function $f(r) \times w(r)$. In fact, η is, to a good approximation, independent of the heliocentric distance for $r > 1.5\ R_\odot$ (remember that the electron temperature, which enters q_{13}, does not vary much and that $G_{13}(r, 0)$ varies little above 1.5 $R_\odot$) and also the Doppler dimming terms D_{12}, D_{13} have a relatively small explicit dependence on it, as already pointed out. Then, for the sake of a simpler discussion, we can describe the variation of ρ with the heliocentric distance by taking η constant and by using the asymptotic expression (eq. [A6]) for the D's. If one furthermore assumes that in the coronal region considered the cross section of a velocity tube increases as r^2 (radial expansion), ρ becomes an explicit function of w only, and its variations with r are brought about solely by the variations of w with r. This includes the effect of the density variations with r, which now affect ρ through w (eq. [11]).

Since η^{-1} is a speed, it can be given a physical meaning by noting that the emissivity ratio can only be significantly different from g_2/g_3 when the outflow speeds are significantly larger than η^{-1}.

A representative value of η for the O VI doublet in a quiet coronal region is 6.61×10^{-7} s cm^{-1}, where we have used the same quantities employed above to get θ [but $h(r) = 1$], and for F the average solar wind value deduced from Schwenn (1983) (proton flux at 1 a.u. = 4×10^8 cm^{-2} s^{-1} and 4% He). For a coronal hole the 60% decrease in the intensity of the lower atmosphere exciting radiation is accompanied by a 50% decrease of F, if we take for this quantity an average value appropriate to high-speed streams (Schwenn 1983). The variations, with respect to the quiet corona value, of T_e and T_k nearly compensate each other, as they do for θ. We therefore get a coronal hole value of η that is about the same as for quiet regions.

The emissivity ratio, calculated with the approximations described above, with the Doppler terms appropriate to the O VI doublet and corresponding to a kinetic temperature of 1.6×10^6 K, is given in Figure 3 for various values of η (*solid*

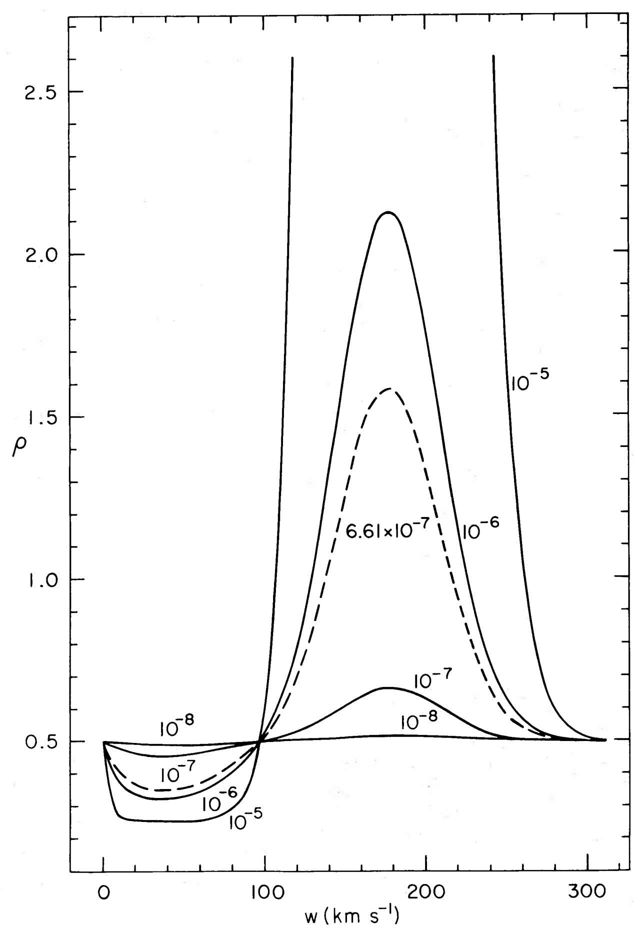

FIG. 3.—The emissivity ratio for the O VI $\lambda\lambda$1032, 1037.6 doublet as a function of the outflow speed w (eq. [14] with the asymptotic form of the D's and $T_k = 1.6 \times 10^6$ K). The numbers on the curves give the parameter η in s cm^{-1}. Dashed curve refers to a standard quiet region and coronal hole (*see text*).

curves), including the value appropriate to the quiet corona (*dashed curve*).

Let us now discuss the curves of Figure 3, interpreting them, on the basis of what has been said above, as representing the variation of the emissivity ratio as the heliocentric distance increases. The variations in the emissivity ratio at low heights (low values of w) are not due to Doppler dimming but simply to variations of the relative importance of the radiative and collisional components. In fact, the lowest coronal point has a finite density value so that $w > 0$; the closer w is to zero, the larger is N_e (eq. [11]) and the closer is the emissivity ratio to the collisional value (eq. [9]). (Obviously $w > 0$ at all heights in an expanding region, where this treatment holds.) With increasing height the flow speed w increases and N_e decreases; thus the importance of the collisional components decreases and so does ρ, until, when w becomes larger than ~ 60 km s^{-1}, Doppler dimming effects reduce the radiation contribution, and the emissivity ratio begins to increase again. When the radiation contribution has decreased to the point where collisional excitation dominates, the emissivity ratio reaches again the collisional value. This occurs at $w \approx 94$ km s^{-1}, independently of η (such that $D_{12} = D_{13} g_3/g_2$). At about $w = 100$ km s^{-1} pumping of coronal O VI ions to the $^2P_{1/2}$ level by the C II chromospheric line becomes important (Fig. 2), with the effect of a rapid increase of the 1037 Å line and of the emissivity ratio. When r is large enough that $w = 172$ km s^{-1} the coronal 1037 Å line absorption profile is centered on the chromospheric C II line; hence a maximum of the emissivity ratio for that heliocentric distance occurs, and subsequently there is a decline that brings ρ again to the collisional value g_2/g_3 when the redshift of the lower atmospheric spectrum in the frame of the coronal O VI ions is so large that the absorption profile relative to the $^2S_{1/2}$–$^2P_{1/2}$ transition is shifted even beyond the C II chromospheric line. Thus the effect of the C II line is that of producing the branches above $\rho = 0.5$ in the curves of Figure 3, which otherwise would stay at $\rho = 0.5$ for the same velocity interval. Hence, for single-line excitation of both components of the doublet, the emissivity ratio would have only the minimum associated with small velocities and would increase to g_2/g_3 at larger heights, such that $D_{12}, D_{13} \to 0$.

If η is large enough that the collisional components become negligible, then the minimum value reached by the emissivity ratio is the radiative limit (eq. [10]). For smaller values of η the densities are larger and the collisional components never become totally negligible, hence the emissivity ratio minimum is intermediate between limits (9) and (10).

Since in the previous discussion w has been considered essentially as a measure of the heliocentric distance through some monotonic function $w(r)$, we need to examine how much this interpretation is influenced by the fact that we have used equation (A6) for the Doppler terms. As Figure 2 shows, the correct Doppler term for $r = 2\ R_\odot$ only differs from the asymptotic one by a $\sim 10\%$ contraction of the scale of the abscissa. Accordingly the correct curves $\rho(w)$ corresponding to the heliocentric distance $r = 2\ R_\odot$ will be obtained from those of Figure 3 by a similar contraction of the scale of the abscissa. At larger heliocentric distances the error brought about by the use of the asymptotic approximation decreases, and so it does at the coronal base where the collisional terms are dominant. Hence, the above discussion remains essentially valid. The assumption $f =$ constant may not be a good approximation in all coronal regions. If not, deviations from a constant value are most likely to occur close to the solar surface, i.e., in the lower velocity region (Munro and Jackson 1977; Munro and Mariska 1977). Therefore the curves of Figure 3 cannot be interpreted as representing the variation of ρ with r in this velocity region for nonradial flow.

Finally, we note that the curves $\rho(w)$ could be sensibly different from those of Figure 3 for a doublet different from the O VI doublet, particularly if the pumping from a nearby line would affect both the $P_{3/2}$ and the $P_{1/2}$ levels.

IV. DETERMINATION OF CORONAL PLASMA PARAMETERS

It is apparent from the preceding discussion that the plasma diagnostic possibilities are greatly enhanced when there is present in the lower atmosphere radiation a nearby spectral line that, when Doppler-shifted by the solar wind, can pump one member of a resonance doublet. In this section we describe how a measurement of just the intensity ratio of the doublet as a function of height can be used to set limits on coronal values of particle flux and outflow speed. In some cases the values of these quantities can be obtained without reference to other parameter determinations. We also describe how the outflow velocity can be obtained from a measurement of the intensity ratio and an independent measurement of electron density (e.g., from Thompson scattering) or from knowledge of the particle flux. The diagnostics derived from the resonance doublet have the further advantage that the intensity ratio does not depend on the ionization balance of the ionic species and that the doublet levels, in this case, are populated only via excitations from the ground level. This makes its population the only one to enter the intensity formulation (see § III). Doublets also have the advantage that the radiometric calibration of an instrument is usually about the same for both lines.

Although we will illustrate this category of diagnostics with the O VI doublet at $\lambda\lambda 1032$, 1037.6 (where the latter can be pumped by C II $\lambda 1037.0$), it is clear that a similar treatment can be applied to the other doublets listed in § I.

In the following we distinguish between two categories of the diagnostics: the first is based almost entirely on the measured intensity ratio of the doublet, and the other requires, in addition, an independent knowledge of electron density or particle flux. The latter category is further divided into discussions of high- and low-speed regimes. As in § III the following ignores initially the complication (Kohl *et al.* 1983) of the line-of-sight contribution. For some narrow coronal structures (such as streamers and transients) the emissivity ratio is nearly equal to the measured intensity ratio (see § III). In the case of broader structures (such as coronal holes) this approximation is less accurate, but only a very inexact coronal model is needed to take the line-of-sight effects into account. In the following we continue to assume that the emissivity ratio is a measurable quantity (i.e., the intensity ratio).

a) Information from Only the Measured Intensity Ratio

Figure 3 can be used to illustrate the information to be gleaned from just the doublet emissivity ratio ρ. (In an actual application more exact curves obtainable from eq. [14] should be used, which employ the values of the D factors as a function of heliocentric distance rather than the asymptotic forms used for Fig. 3.)

It is clear from Figure 3 that a determination of the emissivity ratio at a single heliocentric distance in a coronal structure is sufficient to put limits on the outflow speed w and the quantity η which is inversely proportional to the particle flux. The limit on η is a lower bound that corresponds to the curve that has the measured value of ρ at the peak (if $\rho > 0.5$) or at the minimum (if $\rho < 0.5$): for example, if $\rho = 2.1$ then $\eta > 10^{-6}$ s cm^{-1}. The limit on w is insensitive to the value of η. If $\rho > 0.5$ then $w > 94$ km s^{-1} and if $\rho < 0.5$ then $w < 94$ km s^{-1}. Information of this kind can be very important. For $\rho > 0.5$ it would provide a check on the presence of large outflow values derived from the observations of Lyα, and for $\rho < 0.5$ it identifies regions where there is no significant Doppler dimming of Lyα so that the Lyα intensity is a measure of the H I density.

More stringent limits on w and η can be obtained if the intensity ratio is measured at more than one heliocentric distance along a radial direction in a single coronal structure (so that the assumption of constant T_e and therefore of constant η is approximately valid). In this case the values of ρ should be found to follow one of the curves of Figure 3. In particular, if ρ is determined continuously from the base of a coronal structure to large heliocentric distances, it should often be possible to observe the expected excursion through the peak value of ρ and the subsequent decline at larger heights. This effectively identifies the curve in Figure 3 that is appropriate for the observed region and hence provides values of the outflow velocity as a function of height and also the value of η. (The same occurs if ρ is observed to go through a minimum; note, however, that the identification of the curve is more difficult if the minimum value of ρ is not significantly larger than 0.25.)

It should be noted that the curves in Figure 3 provide two values of w for each value of ρ, but when ρ is measured over a range of heights the choice of the smaller versus the much larger value of w at each height should be obvious. For example, if ρ is determined at several heights but no peak is observed, then the highest value of ρ (if $\rho > 0.5$) sets the limit on η. The observations at other heights now set limits on w. Suppose that two observations have yielded $\rho = 2.1$ and $\rho = 1.5$, respectively, then $\eta \geq 10^{-6}$ s cm^{-1} and the value of w at the height corresponding to $\rho = 1.5$ is limited between 94 and 150 km s^{-1} or is larger than 212 km s^{-1}. If the observation where $\rho = 1.5$ corresponds to a heliocentric distance that is larger than that of the observation where $\rho = 2.1$, then the second limit is valid; otherwise the first one is applicable. For the value of w at the height corresponding to $\rho = 2.1$, we have the same limit as before ($w > 94$ km s^{-1}).

b) Further Information Provided by Other Observations

i) *The Case of High Outflow Speeds*

Obviously the situation is even better if other empirical data also exist. If η were known then the uncertainty on w arising from a single measurement of ρ would be reduced to two values, both of which would be consistent with the doublet emissivity ratio. Measurements of ρ at several heliocentric distances within the coronal structure would be expected to provide sufficient information to choose between the two possible values.

It is likely that supplementary information will concern N_e rather than the particle flux F and therefore that θ will be known rather than η. (The value of F can be obtained by "in situ" measurements in the interplanetary space; however, these measurements should refer to the same magnetic tube to which the coronal EUV measurements refer. In practice, one would be compelled, in most cases, to use average values for F.) To study this case we plot in Figure 4 the emissivity ratio given by equation (8), as a function of w, where θ, as defined by equation (6), depends primarily on N_e (see § III for representative values of θ for O VI. For the Doppler dimming terms we use the asymptotic expression (eq. [A6]), as we did above.

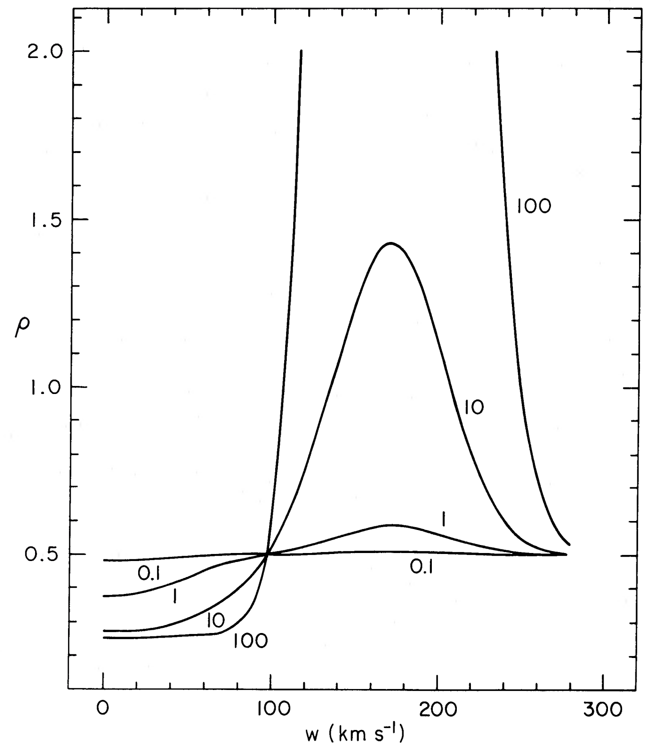

FIG. 4.—Same as Fig. 3 but having θ instead of η as a parameter (eq. [8])

Because the curves of Figure 4 cannot be interpreted as representing the variation of the emissivity ratio with heliocentric distance (as were the curves of Fig. 3), different curves for different values of the parameter θ must be used at each heliocentric distance.

Having θ (from N_e and T_e) and using a graph like those of Figure 4 at a series of heliocentric distances in a chosen coronal structure, two possible values of w will be found at each height where $\rho > 0.5$. (The case of low velocities, $\rho < 0.5$, is discussed in § IV*b*[ii]). Again, an inspection of the possible values of w for a range of heights will almost certainly yield an obvious choice between the large and small velocity value at each observed point.

Up to this point we have assumed that the extent of the observed coronal structure is small enough, along the line of sight, that the doublet emissivity ratio is nearly equal to the observed intensity ratio. In order to represent better the line-of-sight variations and hence refine the measured outflow velocities, the results of the preceding analysis should be introduced as initial values into a detailed coronal model which would also contain measured values of other coronal parameters such as N_e, T_e, and T_p. The measured doublet intensity ratio then becomes the constraint on the model that tends to be most sensitive to outflow velocity and, unlike the intensities of the individual lines, it is insensitive to the chemical abundance and the ionization balance of the ion considered.

ii) *Measurements of Low Outflow Speeds*

As discussed in § IV*a*, regions of low outflow speed ($w < 94$ km s^{-1}) can be identified as those having $\rho < 0.5$. In these regions one can still use the curves of Figure 4 to get information on w from the emissivity ratio, if θ is known. This procedure is equivalent, for $w < 80$ km s^{-1}, to the one proposed by Kohl and Withbroe (1982); this arises from the fact that in the low-speed regime the Doppler dimming of both members of the doublet is the same (see Fig. 2), since in this case the neighboring line has no effect. Hence, putting $D_{12} = D_{13}$ in equation (8), it can be solved for θD_{13}, which is the ratio between radiative and collisional components considered by Kohl and Withbroe. The outflow speed can then be determined in terms of the emissivity ratio and other measurable quantities [i.e., mainly N_e and G_{13} $(r, 0)$]. Like the high-speed case, the ionization balance of oxygen need not be known.

Figure 4 shows that in the extreme case $\rho \approx 0.25$ the emissivity ratio is insensitive to outflow speed, so that, for the latter, one can only obtain the upper limit $w < 94$ km s^{-1} from the ratio. This corresponds to the collisional components of the doublet lines being much smaller than the radiative ones, so that the Doppler dimming terms cancel in the emissivity ratio.

In this case the correct procedure would be that of using the absolute intensity of the lines rather than the intensity ratio and thus deduce the resonantly scattered component of, for example, the 1–2 line as

$$\int_{-\infty}^{\infty} j_{12}\, dx = I_{13}/2 - I_{12} \; .$$

According to equation (2), the resonantly scattered component can be written as

$$j = \text{const } A_{\rm el} RG(r, 0) N_e \mathrm{D}/r^2 \; ,$$

where $A_{\rm el}$ is the chemical abundance of oxygen and R is the ionization balance term, which depends primarily on the electron temperature. With an appropriate value of this quantity and an independent determination of N_e (e.g., from Thomson scattering) and G (from a UV observation of the solar disk) the Doppler dimming term can then be obtained. This quantity, as Figure 2 shows, is sensitive to velocity, which can then be determined in this way.

Insensitivity to w arises also for $\theta \ll 1$, i.e., when the collisional components of the doublet lines are dominant. However, this possibility is not of concern in coronal regions of interest for the O VI doublet, since $\theta \ll 1$ in regions where w is expected to be negligible (in quiet or active regions and coronal holes at very low heights; see § III).

V. CONCLUSIONS

We conclude that a rather powerful tool for investigating the wind source regions in the extended corona is provided when a neighboring spectral line is present which can pump one member of a Li-like or Na-like resonance doublet of a coronal ion. This is the case for resonance scattering by coronal O VI λ1032 and λ1037.6 because of the C II λ1037.0 line in the chromospheric radiation and is also the case for other doublets. Particularly in the case of coronal structures that only extend a relatively small distance from the plane of the solar disk but also, less accurately, for extended structures, the doublet intensity ratio can identify regions where the outflow velocity is greater than or less than 94 km s^{-1}. In many cases the ratio can specify both the outflow velocity and, if the exciting radiation is measured, the value of the outflowing particle flux. If independent knowledge of N_e exists, then a rather accurate determination of outflow velocities in the 30–250 km s^{-1} range is obtainable. This method for determining heavy ion outflow is independent from Doppler dimming of H I Lyα.

The O VI doublet appears to provide the best suitable diagnostics for determining low outflow velocities in the 30–80 km s^{-1} range. This capability is expected to prove invaluable in the investigation of the source region of the low-speed solar wind.

In order to refine the values of outflow velocity determined directly from the doublet intensity ratio and to take the line-of-sight effects into account, those values should be used as starting points in a detailed coronal model, and the doublet intensity ratio then becomes the constraint on the model that primarily controls the outflow velocity. In the above discussion, for the sake of simplicity and clarity, we have used several approximations that would not be used in the interpretation of observational data.

This work has been supported by NASA grant NAG5-613 to the Smithsonian Astrophysical Observatory and by Consiglio Nazionale delle Ricerche of Italy.

APPENDIX

THE EMISSIVITY OF A RESONANTLY SCATTERED SPECTRAL LINE

We calculated here the emissivity in a coronal line due to resonant scattering. A photon having frequency ν' in the frame where the emitting atmosphere is at rest is seen by an ion moving with the velocity $\boldsymbol{v}$ at the frequency ν given by:

$$\nu' = \nu\left(1 + \frac{\boldsymbol{v} \cdot \boldsymbol{n}'}{c}\right), \tag{A1}$$

where $\boldsymbol{n}'$ is the unit vector parallel to the velocity vector of the incident photon and c is the light velocity. If ν_0 is the frame of rest frequency of the line considered, the number of absorptions per unit volume and per second due to radiation incident on the scattering ions along direction $\boldsymbol{n}'$ will therefore be given by

$$\int_{\infty} N_1 f(\boldsymbol{v}) d^3 v \int_0^{\infty} B_{12}\, \psi(\nu - \nu_0)\left[\mathscr{I}(\nu', \boldsymbol{n}')\, \frac{d\omega'}{4\pi}\right] d\nu \; ,$$

where B_{12} is the Einstein coefficient for absorption, $\mathscr{I}(\nu', \boldsymbol{n}')$ the exciting intensity at the frequency ν' (given by eq. [A1]), $d\omega'$ the infinitesimal solid angle around $\boldsymbol{n}'$, N_1 the number of absorbing ions in the ground level per cubic centimeter, $f(\boldsymbol{v})$ the distribution function of these in velocity space and $\psi(\nu - \nu_0)$ the absorption profile. Since, in coronal conditions, the frequency spread associated with the velocity spread of the scattering ions is much larger than that associated with $\psi(\nu - \nu_0)$ we can approximate the latter with a δ-function.

At the low coronal densities all absorbed photons are reemitted via spontaneous decay. If we are interested in the total intensity (i.e., integrated over the line width) of the scattered radiation, we do not need to distinguish between the frequencies of the emitted photons: they all contribute to the intensity of the scattered line with virtually the same energy $h\nu_0$. Accordingly, the total emissivity in the line along direction n due to scattering is given by

$$j(P, \boldsymbol{n}) = \int_\Omega p(\phi)d\omega' B_{12} \frac{h\nu_0}{4\pi} N_1 \int_\infty \mathscr{I}(\nu_0 + \delta\nu, \boldsymbol{n}')f(\boldsymbol{v})d^3v ,$$

where P is the coronal point considered, ϕ is the angle between $\boldsymbol{n}$ and $\boldsymbol{n}'$, Ω is the solid angle subtended by the region where the exciting radiation originates, and $p(\phi)d\omega'$ is the probability that a photon traveling along $\boldsymbol{n}$ would have been in $d\omega'$ before scattering (Fig. 1). The quantity $\delta\nu = \nu_0(\boldsymbol{v} \cdot \boldsymbol{n}')/c$ is the Doppler shift of the exciting radiation for the observer at rest with respect to the scattering ion.

If the distribution of the scattering ions is Maxwellian in the velocity space around a point $\boldsymbol{w}$, then in any system of orthogonal coordinates $v_p, v_q, v_r, f(\boldsymbol{v}) = g(v_p - w_p)\, g(v_q - w_q)\, g(v_r - w_r)$. Thus one can take the p-axis along $\boldsymbol{n}'$ and integrate to give

$$j(P, \boldsymbol{n}) = B_{12} \frac{h\nu_0}{4\pi} N_1 \int_\Omega p(\phi)d\omega' \int_{-\infty}^{\infty} \mathscr{I}[\nu_0 + \delta\nu(v_p), \boldsymbol{n}']g(v_p - w_p)dv_p . \tag{A2}$$

The vector $\boldsymbol{w}$ introduced above represents the mean velocity of the coronal ions in the point considered. Its being not zero introduces a dependence on the direction because $w_p = \boldsymbol{w} \cdot \boldsymbol{n}'$ depends on $\boldsymbol{n}'$. A further dependence on the direction of the inner integral in equation (A2) is due to the fact that both the transition region and the chromosphere are not uniformly bright, which is expressed by the explicit dependence of the exciting intensity on $\boldsymbol{n}'$.

By a convenient transformation the variable of the inner integral in equation (A2) can be changed into wavelength, λ, giving:

$$j(P, \boldsymbol{n}) = B_{12} \frac{h\lambda_0}{4\pi} N_1 \int_\Omega p(\phi)d\omega' \int_0^\infty I(\lambda - \delta\lambda, \boldsymbol{n}')\Phi(\lambda - \lambda_0)d\lambda , \tag{A3}$$

where the function $I(\lambda, \boldsymbol{n}')$ gives the exciting intensity per unit of wavelength as measured by an observer at rest and Φ is the transformation of g, i.e., it is the normalized absorption profile whose width is due to the velocity spread of the absorbing ions. The laboratory wavelength of the transition considered is $\lambda_0 = c/\nu_0$, and $\delta\lambda = \lambda_0 w_p/c$; thus $\delta\lambda$ depends on w_p, and hence on the direction of the incoming radiation.

It is possible to find approximate expression for j. To do this we first examine the factor $p(\phi)$. This factor includes a small dependence on the direction of $\boldsymbol{n}'$ which changes from line to line. For the $2s$–$2p$ transition, when the two P levels are well separated, its form is

$$^2S_{1/2} - {}^2P_{3/2} , \qquad 4\pi p(\phi) = (7 + 3\cos^2\phi)/8 ;$$
$$^2S_{1/2} - {}^2P_{1/2} , \qquad 4\pi p(\phi) = 1 .$$

The combination of these two, when the two lines are not resolved, gives

$$4\pi p(\phi) = (11 + 3\cos^2\phi)/12 ,$$

which has been used for Lyα by Beckers and Chipman (1974) (Landi Degl'Innocenti, private communication). In any case, the p factor does not differ much from $1/4\pi$. For example, in the worst case ($^2S_{1/2} - {}^2P_{3/2}$), along the line of sight having $r = 2\,R_\odot$ as the minimum heliocentric distance ($R_\odot$ is the solar radius), $4\pi p$ varies at $x = 0$ (x defined in § II) from $\frac{7}{8}$ for radiation coming from directly underneath to 0.97 for radiation coming from the limb; at $x = \pm 2\,R_\odot$ $4\pi p$ varies from 0.94 to 1.19; larger values of x should correspond to considerably lower density, at least in a spherically symmetric corona, so that their contribution to the observed intensity should be negligible. Hence a good approximation for a mean value of p is $p = 1/4\pi$.

If we now add the approximation that $\boldsymbol{w}$ is parallel to $\boldsymbol{r}$ and that the lower atmosphere is uniformly bright in the exciting radiation, j becomes a function of r and w only. Accordingly the quantity G defined in equation (3) can be written

$$G(r, w) = \frac{r^2}{4\pi} \int_\Omega d\omega' \int_0^\infty I(\lambda - \delta\lambda, \boldsymbol{n}')\Phi(\lambda - \lambda_0)d\lambda ,$$

whence

$$D(r, w) = \frac{G(r, w)}{G(r, 0)} .$$

We turn now to the angular dependence contained in $\delta\lambda$. Since $\delta\lambda$ depends on w_p it depends on the direction of the incoming radiation. For radial outflow the Doppler effect that causes the shift is maximum for the radiation originating in the lower atmosphere directly below the point P and is minimum for that originating at the solar limb. The difference becomes larger as the heliocentric distance of P gets smaller; if this is $2\,R_\odot$ the angle between $\boldsymbol{w}$ and $\boldsymbol{n}'$ for radiation coming from the solar limb is 30°, whence $w_p = 0.87w$ for radiation coming from the solar limb, while $w_p = w$ for radiation from the solar point directly below P. The value of $\delta\lambda$ in equation (A3) will then differ from the asymptotic (corresponding to $r = \infty$) value, $\delta\lambda_0 = \lambda_0 w/c$, at most by 13% for

$r = 2\ R_\odot$ and less at larger r. Even less will differ the mean $\langle \delta\lambda \rangle$. Nevertheless, even a small difference in this quantity can cause a considerable difference in G if Doppler dimming is strong. However, the substitution for $\langle \delta\lambda \rangle$ of its asymptotic expression, consisting of the use of w for the mean of w_p over the solid angle Ω, will not alter the general form of G as a function of w, but simply cause a few percent contraction of the scale of the abscissae. To check this we have illustrated in Figure 2 the Doppler terms D for radial flow and uniform exciting intensity, calculated in the point P having $r = 2\ R_\odot$ and $x = 0$ (i.e., $P = P_0$), both with the exact expression (eq. [4]) and with the approximate one (eq. [A6]) (which includes the asymptotic form for $\langle \delta\lambda \rangle$). Figure 2 confirms that the effect of the use of the approximate expression (eq. [A6]) is that of introducing a contraction of the scale of the abscissae, which amounts to $\sim 10\%$ for $r = 2\ R_\odot$.

Before integrating over ω' we write the solid angle Ω as

$$\Omega = \frac{\pi R_\odot^2}{r^2}\, h(r)\ ,$$

where the function $h(r) = 2[1 - (1 - R_\odot^2/r^2)^{1/2}]r^2/R_\odot^2$ decreases between 2 for $r = R_\odot$ and 1 for $r = \infty$. If we then use for Ω the asymptotic expression $\pi R_\odot^2/r^2$, this will cause an underestimation of G which is a factor of 2 at $r = R_\odot$, but only 15% at $r = 1.5\,R_\odot$, 7% at $r = 2\ R_\odot$, and still smaller at larger heights.

We then have the approximate expression

$$G(r,\, w) = \frac{R_\odot^2}{4} \int_0^\infty I(\lambda - \delta\lambda_0)\Phi d(\lambda - \lambda_0) d\lambda = \frac{R_\odot^2}{4}\, h(r) F(\delta\lambda_0)\ , \tag{A4}$$

where $F(\delta\lambda_0)$ is the quantity defined in equation (1). Note that for $w = 0$ this approximation does not contain the error due to the use of $\delta\lambda_0$ in place of $\delta\lambda$—hence it is particularly good.

The asymptotic form of the above expression is

$$G(\infty,\, w) = \frac{R_\odot^2}{4}\, F(\delta\lambda_0)\ , \tag{A5}$$

from which

$$\mathrm{D}(\infty,\, w) = \frac{F(\delta\lambda_0)}{F(0)}\ . \tag{A6}$$

REFERENCES

Allen, C. W. 1973, *Astrophysical Quantities* (2d ed.; London: Athlone).
Beckers, J. M., and Chipman, E. 1974, *Solar Phys.*, **34**, 151.
Bely, O. 1966, *Proc. Phys. Soc. London*, **88**, 587.
Jordan, C. 1969, *M.N.R.A.S.*, **142**, 501.
Hyder, C. L., and Lytes, B. W. 1970, *Solar Phys.*, **14**, 147.
Kelly, R. L., and Palumbo, L. J. 1973, *Atomic and Ionic Emission Lines below 2000 Angstroms* (*Naval Res. Lab. Rept.* 7599).
Kohl, J. L., Weiser, H., Withbroe, G. L., Noyes, R. W., Parkinson, W. H., Reeves, E. M., Munro, R. H., and MacQueen, R. M. 1980, *Ap. J.*, **241**, L117.
Kohl, J. L., and Withbroe, G. L. 1982, *Ap. J.*, **256**, 263.
Kohl, J. L., Withbroe, G. L., Zapata, C. A., and Noci, G. 1983, in *Solar Wind Five*, ed. M. Neugebauer (NASA Conf. Pub. 2280), p. 47.
Moe, D. K., and Nicolas, K. R. 1977, *Ap. J.*, **211**, 579.
Munro, R. H., and Jackson, B. V. 1977, *Ap. J.*, **213**, 874.
Munro, R. H., and Mariska, J. T. 1977, *Bull. AAS*, **9**, 370.
Noci, G. 1971, in *Physics of the Solar Corona*, ed. C. J. Macris (Dordrecht-Holland: Reidel), p. 13.
Pottasch, S. R. 1964, *Space Sci. Rev.*, **3**, 816.
Schwenn, R. 1983, in *Solar Wind Five*, ed. M. Neugebauer (NASA Conf. Pub. 2280), p. 489.
Seaton, M. J. 1964, *Planet. Space Sci.*, **12**, 55.
Vernazza, J., and Reeves, E. M. 1978, *Ap. J. Suppl.*, **37**, 485.
Withbroe, G. L., Kohl, J. L., Weiser, H., and Munro, R. H. 1982, *Space Sci. Rev.*, **33**, 17.

JOHN L. KOHL: Smithsonian Astrophysical Observatory, 60 Garden Street, Mail Stop 50, Cambridge, MA 02138

GIANCARLO NOCI: Osservatorio Astrofisico di Arcetri, Largo Fermi 5, 50125 Firenze, Italy

GEORGE L. WITHBROE: Smithsonian Astrophysical Observatory, 60 Garden Street, Mail Stop 15, Cambridge, MA 02138